Journal of Geophysical Research: Atmospheres

Supporting Information for

Decade-long Ozone Profile Record from Suomi NPP OMPS Limb Profiler: Assessment of Version 2.6 Data

N.A. Kramarova[1], P. Xu[2], J.B. Mok[3], P.K. Bhartia[1,*], G. Jaross[1], L. Moy[3], Z. Chen[3], S. Frith[3], M. DeLand[3], D. Kahn[3], G. Labow[3], J. Li[3], E. Nyaku[3], C. Weaver[4], J. Ziemke[5], S. Davis[6], and Y. Jia[6,7]

[1]NASA GSFC, Greenbelt, MD.
[2]SAIC, Greenbelt, MD;
[3]SSAI, Greenbelt, MD;
[4]ESSIC, College Park, MD;
[5]Morgan State University, Baltimore, MD;
[6]NOAA Chemical Sciences Laboratory, Boulder, CO;
[7]Cooperative Institute for Research in Environmental Sciences, University of Colorado at Boulder, CO;
*Emeritus

Contents of this file:

Introduction

We provide 13 additional figures and one table in this supplemental file. These figures and the table are not critical for supporting main conclusions of the manuscript, but we believe readers might find them informative.

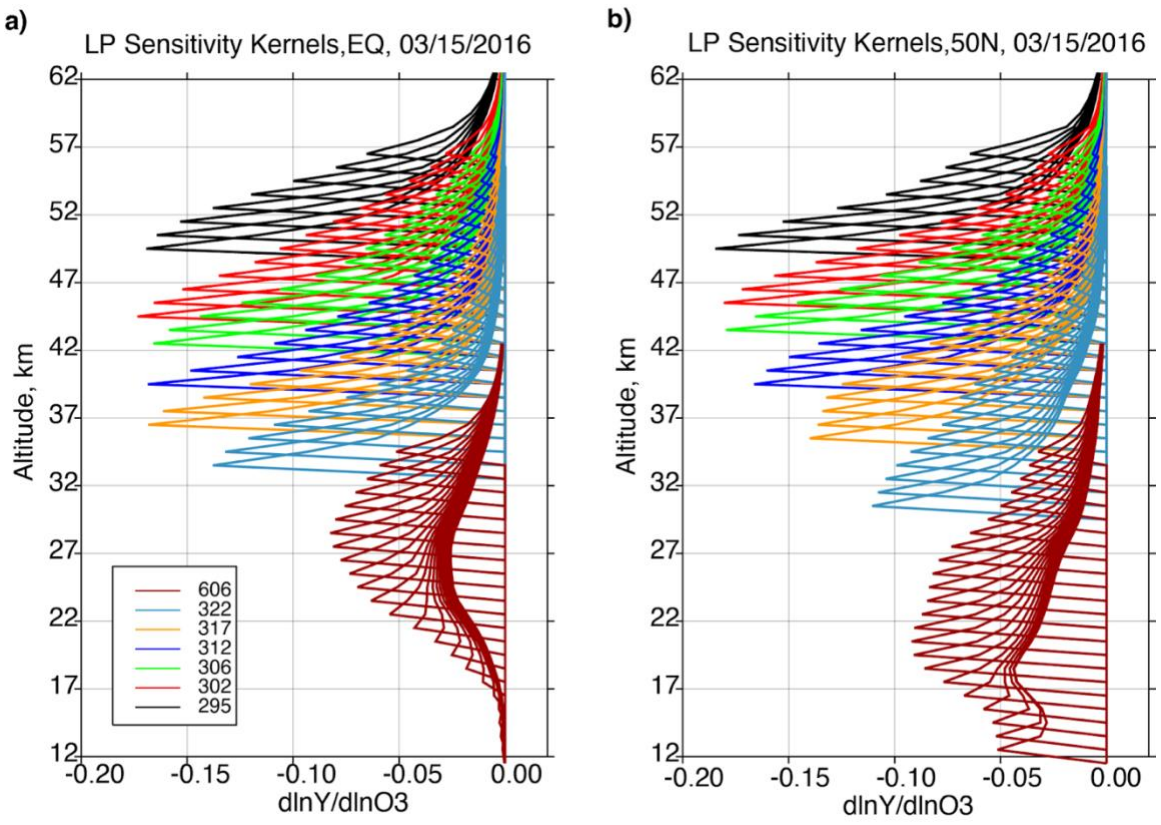

Figure S1. Typical LP sensitivity kernels K=dY(z,λ)/dln(O3) for two cases on March 15, 2016, orbit 22696, events 91 (a) and 156 (b) with coordinates [1N,171E] and [50N,157E], respectively. Kernels for 6 UV pairs and one VIS triplet are shown in different colors. In the tropics, ozone density peak is located higher than in midlatitudes, therefore, we can see that the kernels for VIS triplet and 317 nm and 322 nm UV pairs peak at higher altitudes. Sensitivity of the VIS triplet drops quickly below the ozone peak.

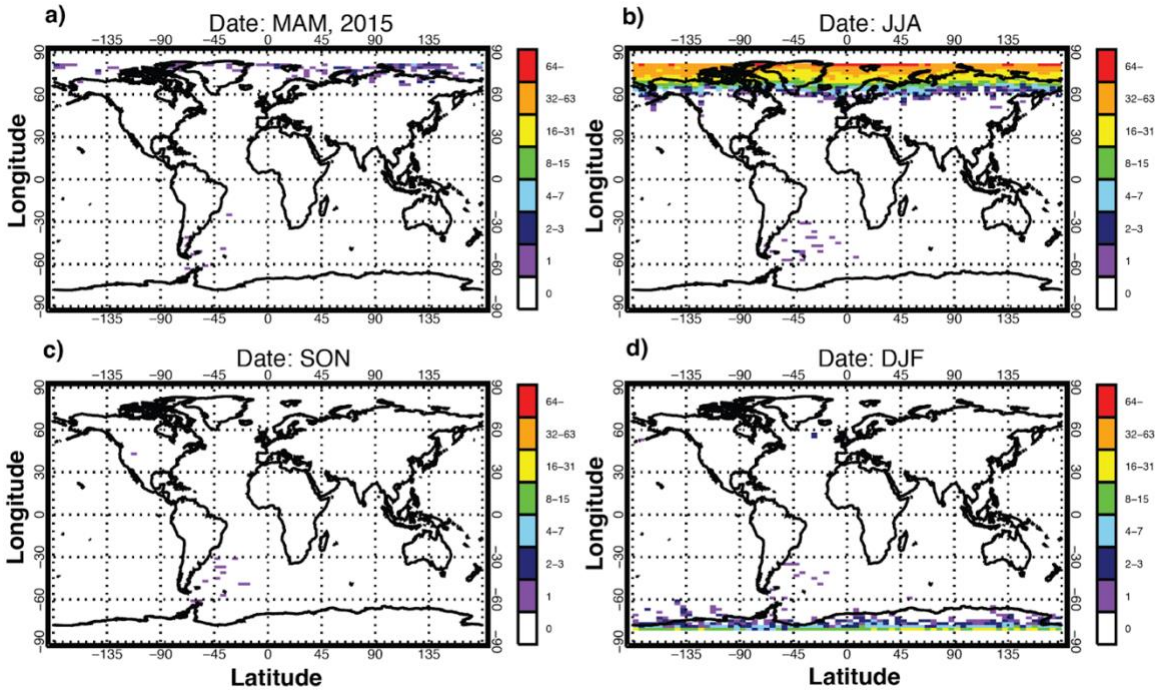

Figure S2. Seasonal distribution of frequency of the PMC flag in 2015: March-April-May, (b) June-July-August, (c) September-October-November and (d) December-January-February. The data are shown in 2 by 5 degrees spatial bins (latitude x longitude) and expressed as the total number of illuminated profiles over the 3-month period. The PMC flag appears more frequently during summer months (b) in the Northern hemisphere and the Southern hemisphere (c). The PMC frequency is greater in the Northern Hemisphere because of the LP viewing conditions: observations in the Northern Hemisphere correspond to the forward scattering and PMC clouds have stronger scattering (increased phase function) in the forward direction.

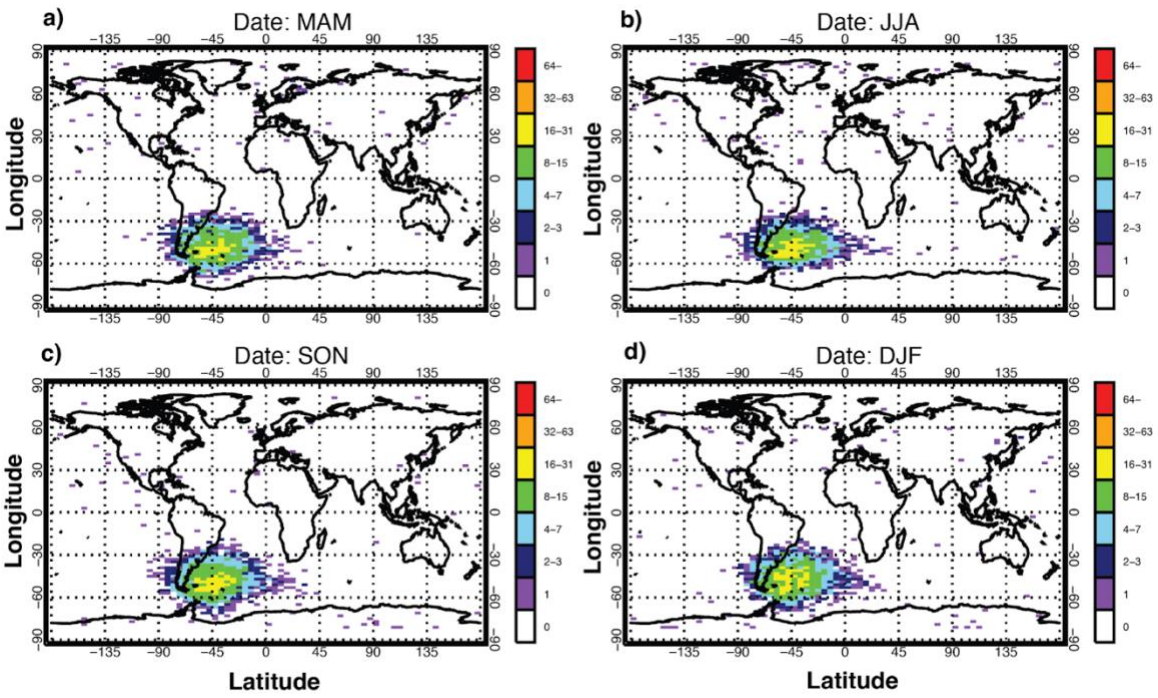

Figure S3. Seasonal distribution of frequency of the QMV flag in 2015: March-April-May, (b) June-July-August, (c) September-October-November and (d) December-January-February. The data are shown in 2 by 5 degrees spatial bins (latitude x longitude) and expressed as the total number of illuminated profiles over the 3-month period. The QMV flag appears more frequently in the Southern Hemisphere over the Atlantic when the satellite flies over the South Atlantic Anomaly. High-energy charged particles contaminate LP measurements. The QMV flag enables us to isolate and remove contaminated measurements. Occasionally the QMV flag occurs in other locations. The frequency of the QMV flag does not change seasonally.

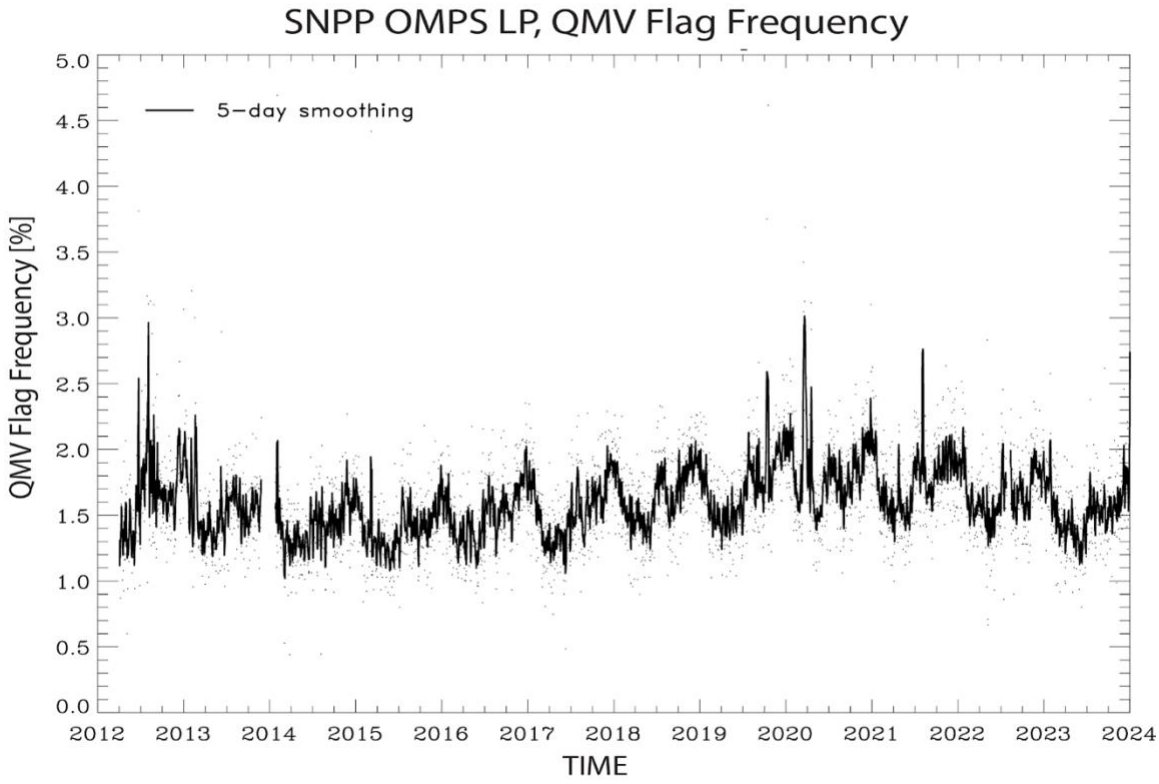

Figure S4. Daily frequency of the QMV flag over the SNPP lifetime. The data are shown as a fraction of data (in %) illuminated by the QMV flag. The frequency of the QMV flag stays around 1-2% and does not change over the instrument lifetime.

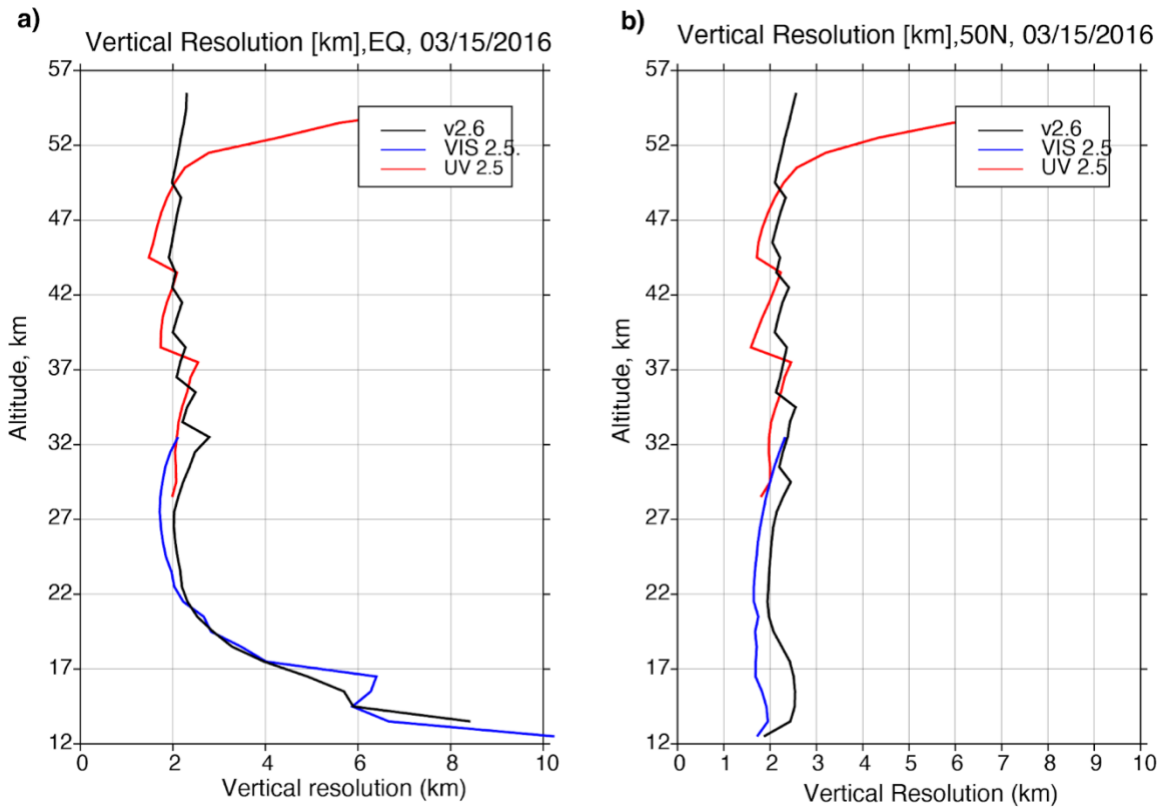

Figure S5. Vertical resolution [in km] of the LP ozone retrievals calculated as the inverse of diagonal elements of the averaging kernel matrix A. Panel (a) shows a typical tropical case, and panel (b) demonstrate a case in mid-latitudes (the same two cases on March 15, 2016, orbit 22696, events 91 (a) and 156 (b) with coordinates [1N,171E] and [50N,157E], respectively, as shown in Fig. A1). Vertical resolution in version 2.6 is shown in black and version 2.5 is shown in red for UV and in blue for VIS retrievals. In version 2.6 the vertical resolution slightly degraded compared to version 2.5 and ranges around 1.9-2.5 km. In the tropic, the algorithm sensitivity below the ozone peak drops sharply leading to a fast degradation of the vertical resolution. Vertical resolution for version 2.5 UV retrievals has sharp changes when the algorithm switches wavelengths. Similar changes are seen in version 2.6 but with a smaller amplitude.

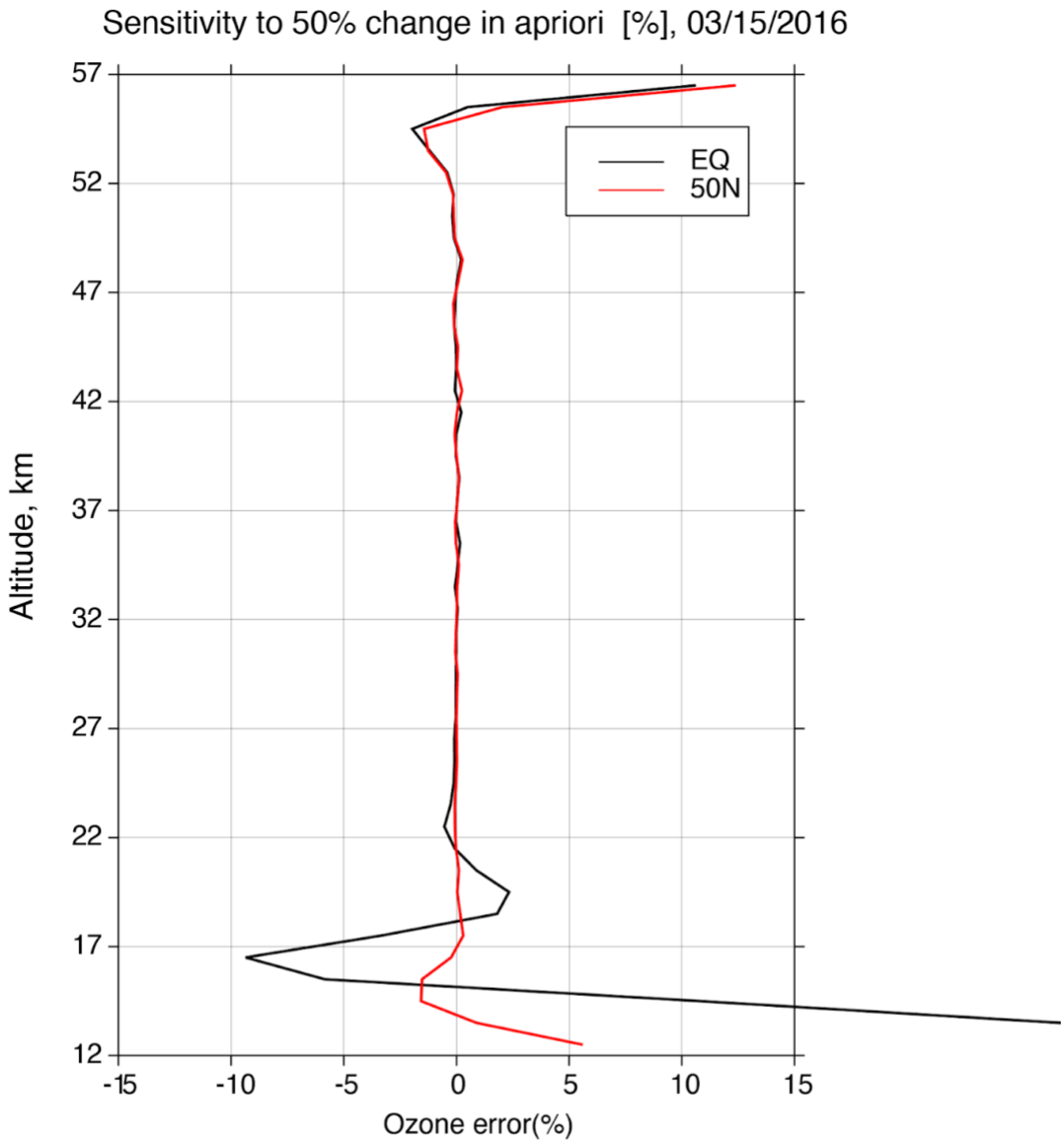

Figure S6. Effects of the apriori error on LP retrievals calculated using the following expression [Rodgers, 2000]: $(I-A)dX_a$ where I is a unit matrix, A – LP averaging kernels, and dX_a is errors in apriori ozone profile. Here we assumed 50% increase in apriori ozone The change is expressed in (%) and shown for the same two cases shown in Figs. S1, S5 and Fig. 5 in the main text (tropics in black and mid-latitudes in red). The LP retrieval algorithm is mainly insensitive to apriori between 17 and 52 km in mid-latitudes and between 22-52 km in the tropics. Sensitivity to apriori increases at the upper and lower portion of the profile where the LP sensitivity kernels (see Fig. S1) sharply declines.

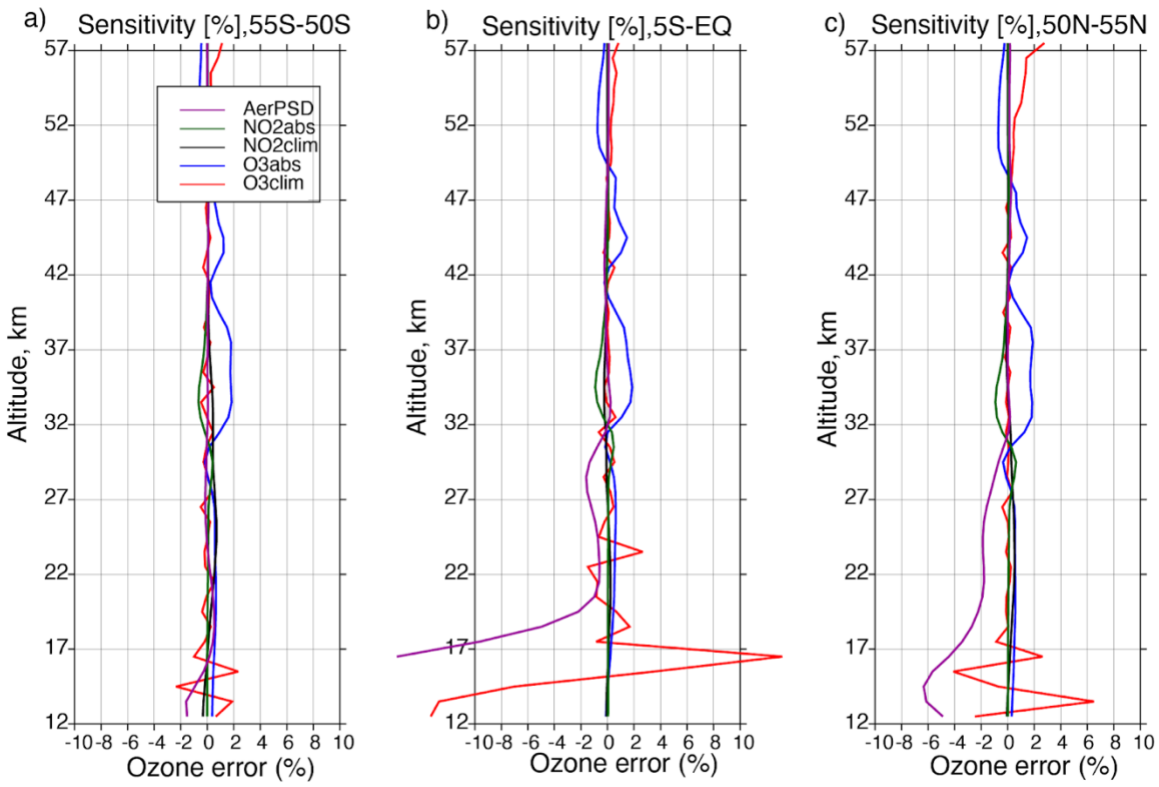

Figure S7. Sensitivity of the version 2.6 LP algorithm to changes in the algorithmic parameters shown for three 5-degree latitude bins on September 23, 2021. Sensitivity are shown for changes in the following 5 parameters: ozone (blue) and nitrogen dioxide (green) absorption coefficients, ozone (red) and nitrogen dioxide (grey) climatologies, and aerosol particle size distribution (purple). Sensitivity is estimated as differences in daily zonal mean ozone between standard retrievals and retrievals with perturbed parameters, which is equivalent to changes in parameters between versions 2.6 and 2.5.

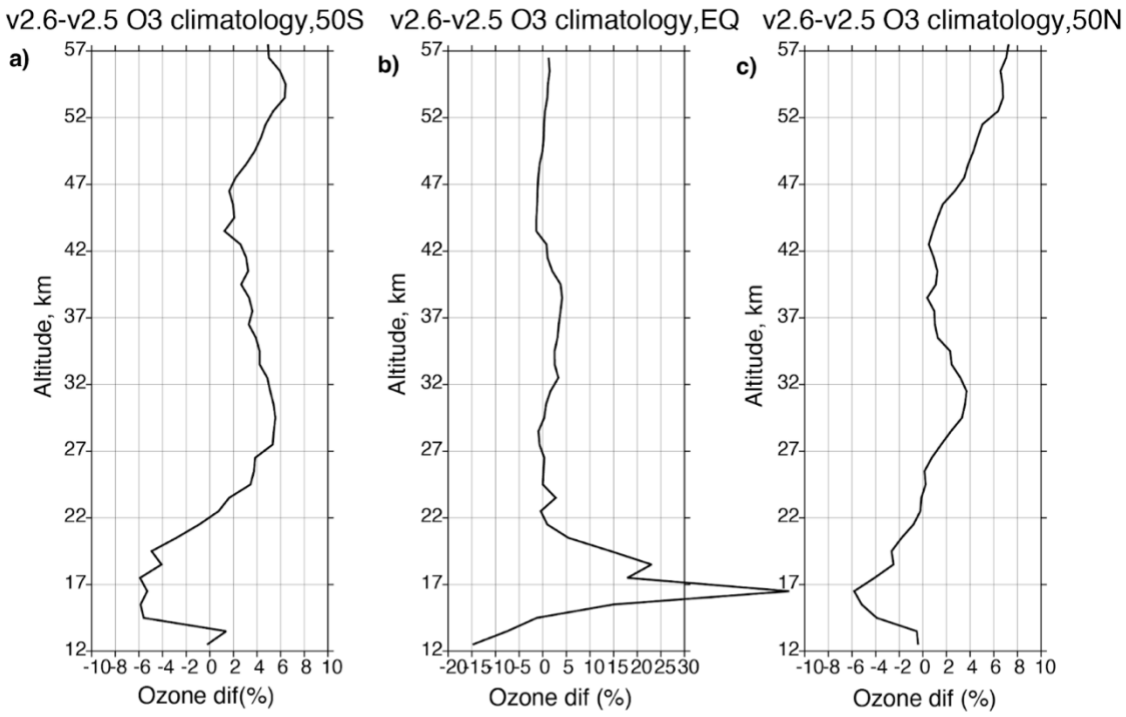

Figure S8. Differences in % between versions 2.6 and 2.5 ozone apriori. The differences are shown for the same 3 latitude bins as in Fig A7. There are oscillations in differences with narrow structures of ~1-km wide. The retrieval algorithm behaves as a low-frequency filter and any fine scale structures that are smaller than the algorithm vertical resolution (in our case 1-km structures) can not be retrieved. Therefore, it is very important to have smooth apriori profiles without sharp vertical gradients. We found that version 2.5 apriori profiles have sharp vertical gradients that lead to observed oscillations in differences.

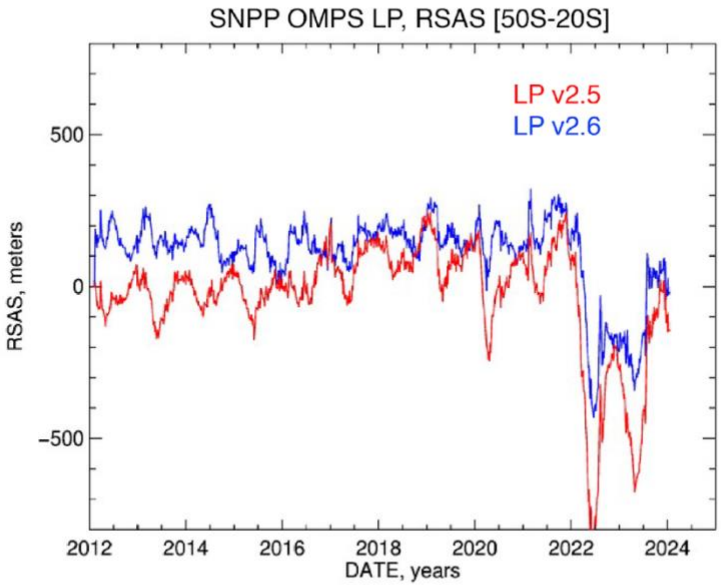

Figure S9. RSAS (Rayleigh Scattering Attitude Sensing) time series for versions 2.5 (red) and 2.6 (blue) from April 2012 through December 2023 in the southern hemisphere (50S-20S). The RSAS method is sensitive to aerosol interference. The Hunga eruption in January 2022 injected large amounts of aerosols into the stratosphere and substantially affected RSAS record (see Sec. 2.2.5). Note that RSAS data in 2022-2023 were not used to determine the corrections for the LP pointing.

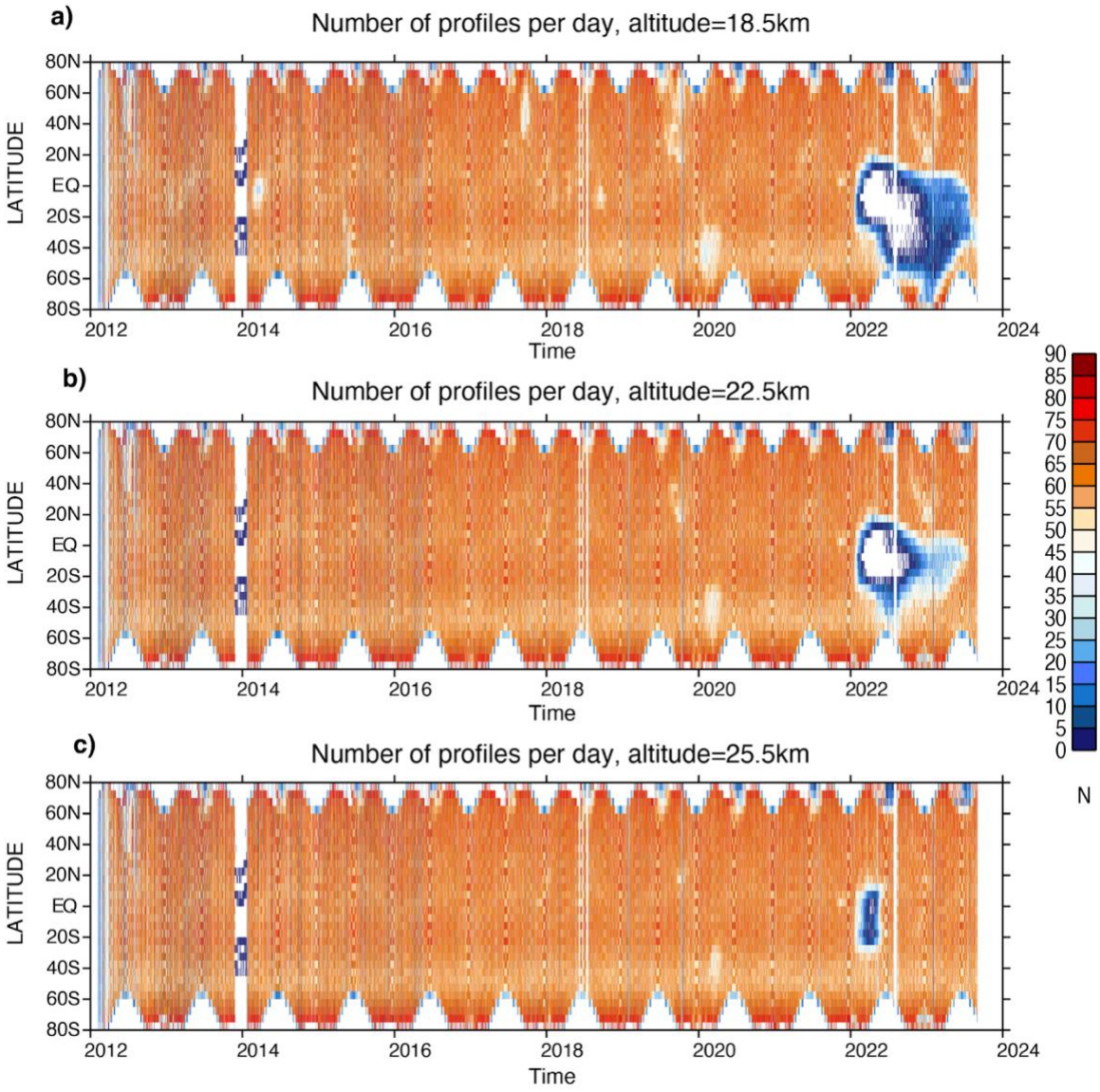

Figure S10. Number of matching LP and MLS profiles in each 5-degree zonal bin daily shown at 3 different levels: (a) 18.5 km, (b) 22.5 km and (c) 25.5 km. After the Hunga eruption in January 2022, the LP profiles were filtered using the concurrent aerosol extinction profiles at 675 nm (see Sec 2.2.5 for details). The number of successful profiles at lowermost stratosphere (18.5 km) in the southern midlatitudes and equatorial latitudes drastically declined leaving gaps in the LP ozone record that lasted for several months. As the aerosol optical depth declines, we see that the number of successful LP observations returns to normal levels. At higher altitudes around 25.5 km, the number of observations in the equatorial zone 20S-20N were reduced for about 6 months, while at 22.5 km there were no observations in the tropics and southern mid-latitudes for about 6-8 months and only after 15 months the number of successful retrievals returned to normal levels.

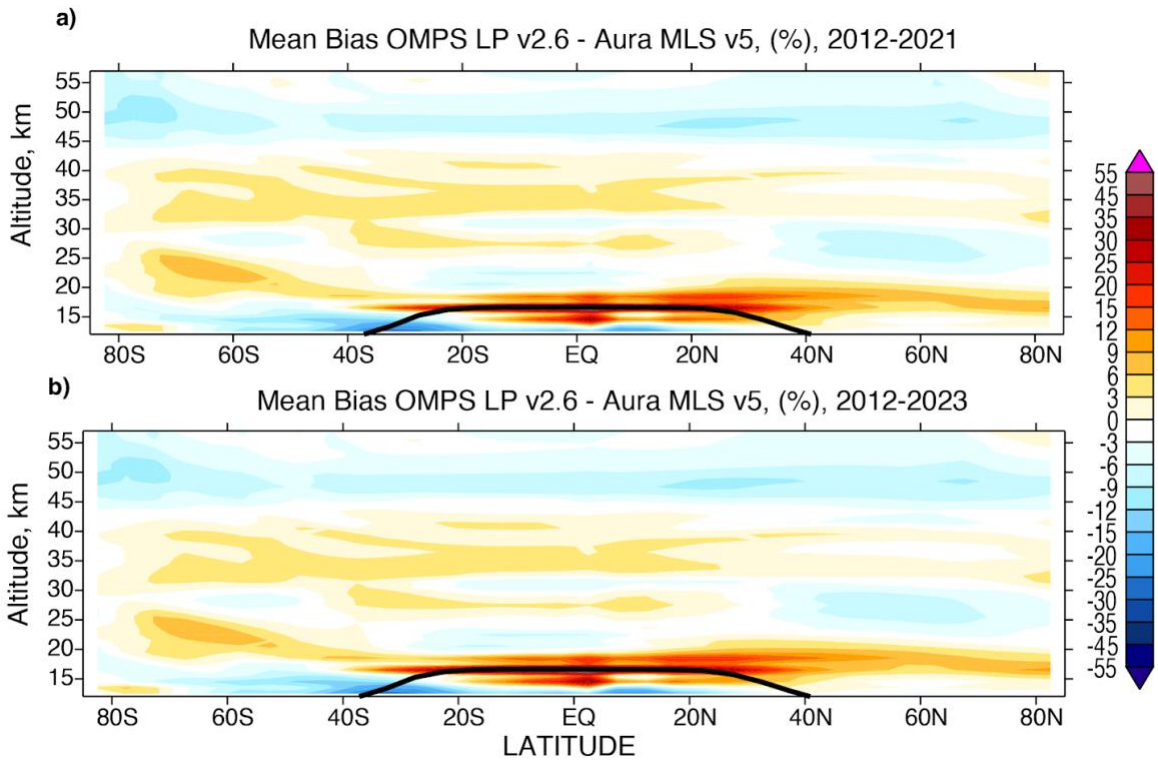

Figure S11. Mean biases between OMPS LP version 2.6 and MLS over 2012-2021 (panel a) and 2012-2023 (b). Mean biases are shown in % as a function of altitude between 12.5 and 57.5 km and latitude (5-degree grid). The black solid line shows the mean tropopause height. The biases did not change due to the extension of the record by two more years.

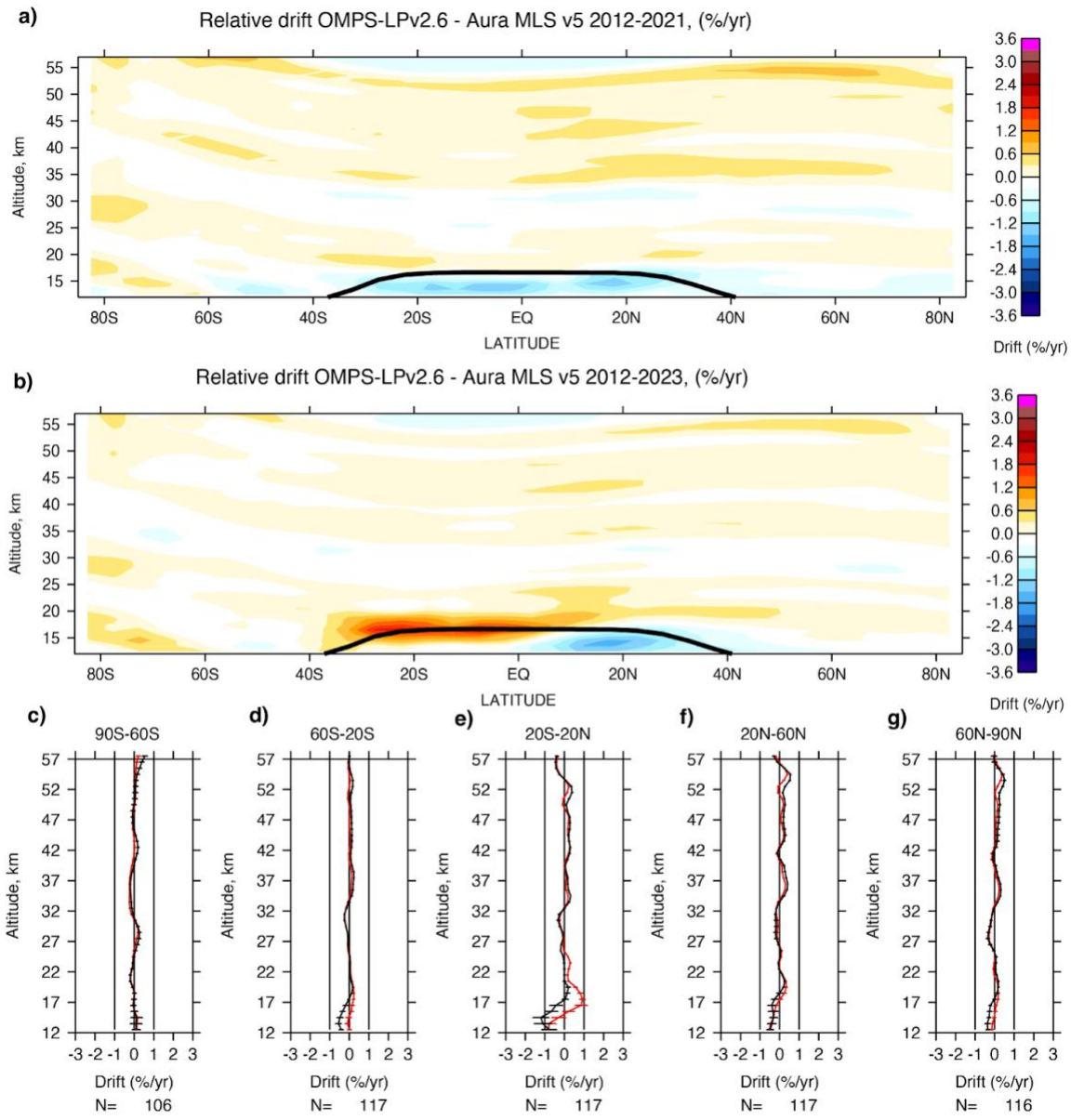

Figure S12. Relative drift between OMPS LP v2.6 and MLS v5 from April 2012 through December 2021 (a) as a function of altitude and latitude (5° latitude grid). Panel (b) is the same as panel (a) but for the period from April 2012 through December 2023. Solid black lines show the mean tropopause height. Panels c-g show vertical structures of the drift in 5 wide latitude bins for 2012-2021 (black lines) and 2012-2023 (red lines). Horizontal error bars show 1σ errors for the linear fit. Extension of the record by 2 more years slightly decreased the relative drift between LP and MLS at higher altitudes above 47 km. However, a strong positive drift appeared in the southern subtropics (40S-EQ) below 20 km, indicating that aerosol from the Hunga eruption led to overestimation of LP ozone in that region after 2022.

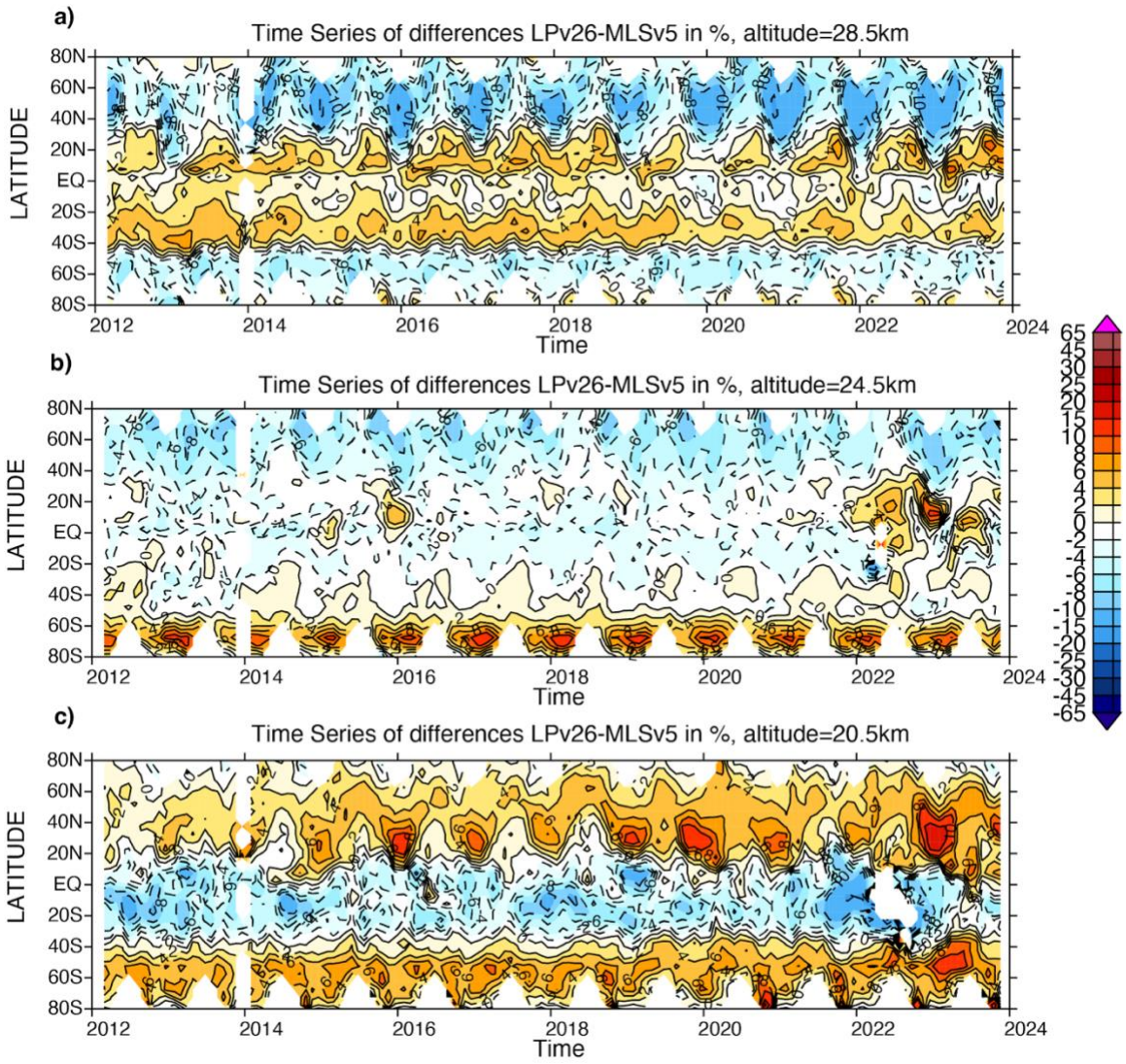

Figure S13. Time series of monthly zonal mean differences in % between LP version 2.6 and MLS version 5 shown as a function of time and latitude (5-degree zonal bins) at 3 different levels: (a) 28.5 km, (b) 24.5 km and (c) 20.5 km. The differences at each level have clear latitudinal and seasonal patterns. After the Hunga eruption in January 2022, the differences tend to increase in the tropics and mid-latitudes. Further investigation is planned.

Wavelength pair/triplet	Normalization altitude	Upper limit	Lower limit
295/353 nm	60.5 km	56.5 km	47.5 - 49.5 km
302/353 nm	60.5 km	56.5 km	44.5 - 46.5 km
306/353 nm	60.5 km	56.5 km	41.5 - 43.5 km
312/353 nm	60.5 km	56.5 km	37.5 – 40.5 km
317/353 nm	60.5 km	56.5 km	33.5 – 36.5 km
322/353 nm	60.5 km	56.5 km	28.5 – 32. 5 km
606/(510&675) nm	40.5 km	35.5 km	12.5 (or cloud top)

Table S1. Vertical range for each UV pair and VIS triplet used in the version 2.6 ozone algorithm. The upper limit and normalization altitude for each pair and triplet are predefined. The lower limit for UV pairs is determined from the vertical shape of measured radiances. For the VIS triplet the lower limit is 12.5 km unless a cloud is detected.